Available online at www.sciencedirect.com
ScienceDirect

International Journal of Refrigeration 30 (2007) 482–488

REVUE INTERNATIONALE DU FROID
INTERNATIONAL JOURNAL OF
refrigeration

www.elsevier.com/locate/ijrefrig

Optimization of finned-tube condensers using an intelligent system[☆]

Piotr A. Domanski[*,1], David Yashar

HVAC&R Equipment Performance Group, National Institute of Standards and Technology, 100 Bureau Drive, Mailstop 8631, Gaithersburg, MD 20899, USA

Received 17 December 2005; received in revised form 11 August 2006; accepted 16 August 2006
Available online 22 November 2006

Abstract

The refrigerant circuitry influences a heat exchanger's attainable capacity. Typically, a design engineer specifies a circuitry and validates it using a simulation model or laboratory test. The circuitry optimization process can be improved by using intelligent search techniques. This paper presents experiments with a novel intelligent optimization module, ISHED (Intelligent System for Heat Exchanger Design), applied to maximize capacity through circuitry design of finned-tube condensers. The module operates in a semi-Darwinian mode and seeks refrigerant circuitry designs that maximize the condenser capacity for specified operating conditions and condenser slab design constraints. Examples of optimization runs for six different refrigerants are included. ISHED demonstrated the ability to generate circuitry architectures with capacities equal to or superior to those prepared manually, particularly for cases involving non-uniform air distribution.

Keywords: Refrigeration system; Air conditioning; Modelling; Optimization; Design; Air condenser; Finned-tube

Optimisation des condenseurs à tubes ailetés à l'aide d'un système intelligent

Mots clés : Système frigorifique ; Conditionnement d'air ; Modélisation ; Optimisation ; Conception ; Condenseur à air ; Tube aileté

1. Introduction

Finned-tube condensers and evaporators are the predominant types of refrigerant-to-air heat exchangers. Their performance is affected by a multitude of design parameters, some of which are limited by the application or available manufacturing capabilities. Once a heat exchanger's outside dimensions, tube diameter, tube and fin spacing, and heat transfer surfaces are selected, the design engineer needs to specify the sequence in which tubes are connected to define the flow path of the refrigerant through the coil, i.e., the refrigerant circuitry. The goal of the design engineer is to specify a circuitry that maximizes coil capacity. The number of refrigerant circuitry options is overwhelming; for example, a three-depth row heat exchanger with 12 tubes per row

[☆] This paper was originally presented at the IIR International Conference, Thermophysical Properties and Transfer Processes of Refrigerants, Vicenza, Italy, August 31–September 2, 2005.

* Corresponding author. Tel.: +1 301 975 5877.
E-mail address: piotr.domanski@nist.gov (P.A. Domanski).
[1] Member of IIR Commission B1.

0140-7007/$35.00 © 2006 Elsevier Ltd and IIR. All rights reserved.
doi:10.1016/j.ijrefrig.2006.08.013

Nomenclature

COP	Coefficient of performance	*Subscripts*	
P	Pressure	Sat	Saturation
Q	Capacity	Sup	Superheat
S	Skew factor – defined in text		
T	Temperature		

has approximately 2×10^{45} possible circuitry architectures. Currently, circuitry design is primarily driven by engineer's experience aided by supplemental heat exchanger simulations, which are performed manually. Designing an optimized refrigerant circuitry is particularly difficult if the airflow is not uniformly distributed over the coil surface. In such a case, the design engineer may be tempted to assume a uniform air velocity profile, which will result in capacity degradation [1].

Among papers considering refrigerant circuitry optimization, an analytical evaluation of the optimum number of parallel sections in an evaporator showed that the maximum capacity is obtained when the drop of refrigerant saturation temperature is 33% of the average temperature difference between the refrigerant and the tube wall [2]. A simulation study of six circuitry arrangements concluded that the heat transfer surface area may be reduced by 5% through proper design of the refrigerant circuitry, compared to common configurations [3]. Another study considering performance of R22 alternatives in condensers demonstrated that different refrigerants require different circuitry architectures to maximize the capacity [4]. The simulation results showed that high-pressure refrigerants are more effective when used with higher mass fluxes than R22 because of their small drop of saturation temperature for a given pressure drop. This conclusion supports the concept of a penalty factor [5], which takes into account a refrigerant's saturation temperature drop during forced convection condensation.

A common aspect of the above studies is that they considered finned-tube heat exchangers with different pre-arranged refrigerant circuitries. A different approach is now possible, through advances made in machine learning, in which customized circuitry designs can be generated for individual heat exchanger applications with uniform and non-uniform inlet air distributions. These capabilities have been demonstrated by a novel optimization system called ISHED (Intelligent System for Heat Exchanger Design) [6]. The follow up work presented the application of ISHED for optimizing refrigerant circuitries in evaporators working with isobutane (R600a), R134a, propane (R290), R22, R410A and R32 [7]. This paper extends the application of ISHED to condensers working with the same six refrigerants, and it constitutes one of the stages of the effort to incorporate ISHED into the heat exchanger simulation package EVAP–COND [8] as a refrigerant circuitry optimization option.

2. Circuitry optimization with ISHED

Fig. 1 presents a general diagram of the ISHED system. It consists of a heat exchanger simulator, which provides capacities of heat exchangers with different circuitry architectures, and a set of modules which participate in the preparation of new architectures. ISHED uses the conventional evolutionary approach in that it operates on one generation (population) of circuitry architectures at a time. Each member of the population is evaluated by the heat exchanger simulator, which provides the heat exchanger capacity as a single numerical fitness value. The designs and their fitness values are returned to the Control Module as an input for deriving the next generation of circuitry designs. Hence, the optimization process is carried out in a loop, and is repeated for the number of generations specified by the user. The user also specifies the number of members in each population at the outset of the optimization run.

The ISHED scheme involves two modules for "breeding" new refrigerant circuitry generations, the Knowledge-Based Evolutionary Computational Module and the Symbolic Learning Module. The Control Module decides which module is utilized to produce the next generation (population). At the outset of an optimization run, the Knowledge-Based Module, which produces designs by applying probabilistically selected circuitry modifying operations to well

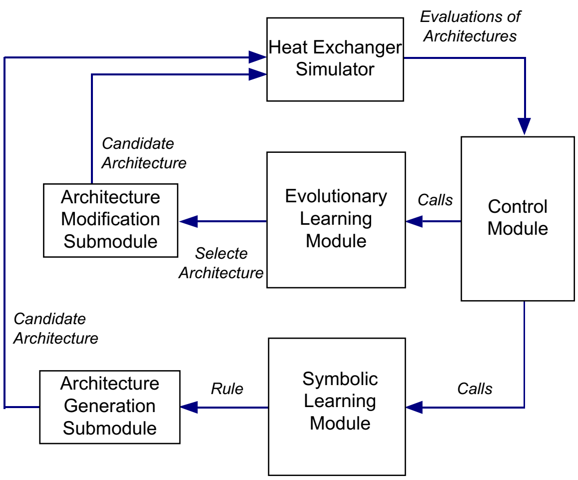

Fig. 1. Functional architecture of ISHED.

Table 1
Refrigerant information[a]

Refrigerant	Saturated vapor pressure[b] (kPa)	Molar mass ($g\ mol^{-1}$)	Molar vapor specific heat[b, c] ($J\ mol^{-1}$)	Safety designation[d]	GWP[e] (100 years horizon)[f]
R600a	604.19	58.122	21688	A3	20
R134a	1159.9	102.03	15392	A1	1320
R290	1534.4	44.096	12808	A3	20
R22	1729.2	86.468	10629	A1	1780
R410A	2729.6	72.585	8622.1	A1/A1	2000
R32	2794.8	52.024	8046.3	A2	543

[a] All fluid properties based REFPROP [12].
[b] Correspond to 45 °C dew-point temperature.
[c] At constant pressure.
[d] From Ref. [13].
[e] Global warming potential.
[f] From Refs. [14,15].

performing designs, is used consecutively until the population's capacities no longer improve. The process then switches to the Symbolic Learning Module, which uses a different approach of hypothesis formation and instantiation for circuitry design, until the performance under this module ceases to improve. The control module alternates between the two modules until a specified number of populations have been examined.

While the overall optimization scheme used by ISHED is consistent with the survival-of-the-fittest Darwinian approach, several aspects of ISHED render it to be classified as non-Darwinian. These aspects include several non-Darwinian operators used in ISHED and their use being restricted by a knowledge domain, and the inclusion of non-Darwinian symbolic learning in the optimization process. More information and references on ISHED are given in the source publication [6].

The condenser simulation model used in this study, COND, was taken from the EVAP–COND simulation package [8]. The most recent validation of the condenser model through laboratory experimentation with R22 and R410A showed the average agreement between measured and simulated capacities to be better than 2% [9]. COND is organized in a tube-by-tube scheme allowing the user to specify arbitrary refrigerant circuitry architectures and a one-dimensional distribution of the inlet air. When the refrigerant in a tube changes from superheated vapor to two-phase flow or from two-phase flow to subcooled liquid, the program locates the transition point and applies appropriate heat transfer and pressure drop correlations to respective sections of the tube. For the purpose of this study, we improved the general robustness of COND (speed and convergence) and upgraded pressure drop correlations for straight tubes [10] and return bends [11].

3. Properties of studied refrigerants

Table 1 presents the refrigerants used in this study. They were selected to provide wide ranges of thermophysical properties that affect heat exchanger and system performance. Differences in thermodynamic properties of the studied refrigerants can be visually recognized on a temperature–entropy diagram, as presented in Fig. 2, with the entropy scale normalized for qualitative comparison. The shown two-phase domes are significantly different, which is chiefly due to different critical temperatures and molar specific heats. Consequently, on a purely theoretical thermodynamic basis, the selected fluids have different coefficient of performance (COP) when evaluated for a vapor compression cycle.

Considering the condenser performance, the location of the critical point and the molar specific heat affect the level of vapor superheat at the condenser inlet. The critical temperature also influences the condenser pressure, vapor density, and the change of saturation temperature with respect to pressure. Among transport properties, liquid thermal conductivity and liquid viscosity are important for heat exchanger performance. Fig. 3 presents these properties for the studied refrigerants relative to the corresponding properties of R22 (where T_{sat} and P denote dew-point temperature and pressure, respectively).

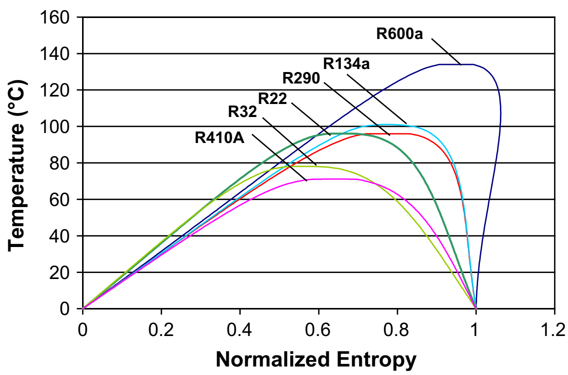

Fig. 2. Temperature–entropy diagram for studied refrigerants (entropy is normalized to the width of the two-phase dome).

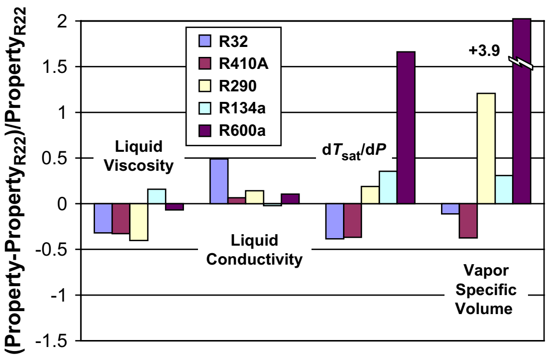

Fig. 3. Thermophysical properties of selected refrigerants relative to R22 properties at 45 °C.

The goal of the heat exchanger design process is to exploit a refrigerant's properties to maximize heat exchanger capacity. This task involves determining the refrigerant circuitry with the optimal mass flux that will benefit the refrigerant heat transfer coefficient at a tolerable pressure drop penalty. Another consideration is the setup of the refrigerant circuit architecture to implement cross-counter flow heat exchange between refrigerant and air. Considering the number of refrigerant properties influencing condenser's performance, finding the optimal circuitry design is a difficult task even for an experienced design engineer.

4. Selected condenser and operating condition

For this study, we used a two-depth row condenser corresponding to a 5.2 kW air conditioning system. Table 2 shows the condenser's design parameters. The air-side operating condition was defined by 35.0 °C inlet air temperature, 50% relative humidity, and 101.325 kPa pressure. The volumetric airflow rate was 0.508 $m^3 s^{-1}$, which produced an average air velocity of 1.0 $m s^{-1}$. The study involved uniform and non-uniform inlet air velocity profiles.

Table 2
Condenser design information

Number of depth rows	2
Number of tubes per row	14
Tube length (mm)	1407
Tube inside diameter (mm)	7.7
Tube outside diameter (mm)	8.3
Tube pitch (mm)	25.4
Tube depth row pitch (mm)	15.9
Tube inner surface	Smooth
Tube material thermal conductivity ($kW m^{-1} K^{-1}$)	0.386
Fin thickness (mm)	0.11
Fin spacing (mm)	1.19
Fin type	Lanced
Fin material thermal conductivity ($kW m^{-1} K^{-1}$)	0.222

Table 3
Condenser inlet refrigerant condition

Refrigerant	Pressure (kPa)	Superheat (K)	Temperature (°C)
R600a	604.2	9.7	54.7
R134a	1159.9	17.8	62.8
R290	1534.4	17.0	62.0
R22	1729.2	33.6	78.6
R410A	2729.6	30.2	75.2
R32	2794.8	46.9	91.9

For all simulation and optimization runs, we kept a constant 45 °C condenser inlet saturation temperature and 5 K subcooling, but used a different inlet superheat for each fluid. We calculated the superheat based upon evaporator exit conditions of 7.2 °C saturation temperature with 5 K superheat, and a compression efficiency of 0.7. This approach for determining the refrigerant state at the condenser inlet has been used in a previous study [4]. Table 3 shows the condenser inlet parameters used. We may note that the value of the condenser subcooling can be optimized to maximize the COP for different refrigerants working in a system; however, the resulting change in the amount of subcooling will have insignificant influence on the circuitry arrangements.

5. Condenser circuitry optimization

Each optimization run with ISHED used 500 populations with 20 members (circuitry designs) per population. Hence, each single optimization run involved the generation and evaluation of 10,000 individual circuitry architectures. Upon completion of the optimization run, we examined the best design and modified it to accommodate manufacturing realities (elimination of overlapping return bends, etc.). We performed two series of optimizations run for: (1) uniform and (2) non-uniform inlet air distribution.

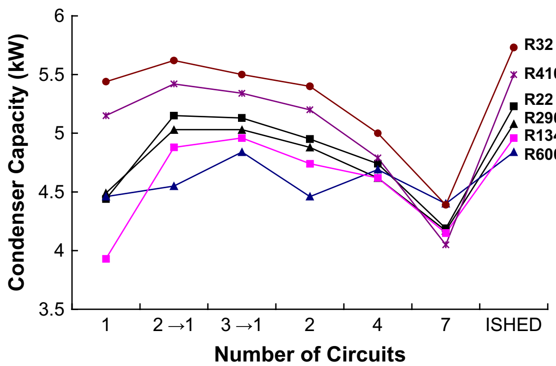

Fig. 4. Condenser capacities for manually developed and ISHED-optimized circuitry designs. 2 → 1 and 3 → 1 denote two and three circuits merging to a single circuit, respectively.

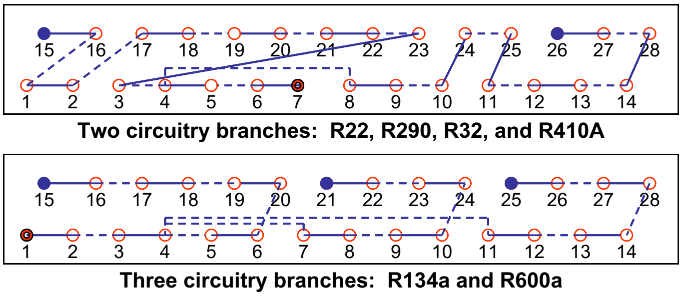

Fig. 5. ISHED-optimized circuitry designs for condensers with two and three circuitry branches.

5.1. Results for uniform inlet air distribution

We started by manually designing 14 different circuitry architectures. These manual designs were of five general types. They consisted of one circuit (2 designs), two circuits converging to a common tube (3 designs), three circuits converging to a common tube (4 designs), two separate circuits (2 designs), four separate circuits (2 designs), and one design with seven separate circuits. We evaluated these designs with COND for each refrigerant, and then performed optimization runs using ISHED. For R290, R22, R32, and R410A, ISHED returned circuitry designs with two circuitry branches merging at a common point. For the other remaining two refrigerants, R134a and R600a, which have a lower saturation pressure than the first group, ISHED designed circuitries with three branches merging at a common point. Fig. 4 shows the results for the best manually designed circuit architectures and for the architectures optimized by ISHED. In each case, the ISHED design was better than or equal to the best manually designed circuitry paths.

With knowledge of the fluid properties, it seems logical that the studied fluids have the relative assortment of configurations shown in Fig. 4. R600a tends to be more adversely affected by increases in mass flux, and seems to benefit from more parallel circuits than the other refrigerants. The opposite is true for R32. ISHED does not know this at the onset of the optimization run, but it learns that certain attributes tend to produce more favorable results and it propagates these features from one generation to the next.

We may note that, although the ISHED-optimized circuitries were unique to their respective refrigerants, designs of a given type were fairly similar to one another, and each refrigerant performed approximately the same in circuitries of the same type. Fig. 5 shows two designs that are characteristic of the two design groups.

Another observation can be made that the ranking of refrigerants shown in Fig. 4 corresponds to the order of their saturation pressure, i.e., the high-pressure refrigerants are better performers than the low-pressure counterparts. The capacity spread between the high-pressure R32 and low-pressure R600a is 18%. In general, the obtained ranking of performance agrees with the ranking reported in a similar evaporator study, shown in Fig. 6 [6]. (The exception is the shift in relative performance of R22 and R290, which can be explained by the relative change in influential properties of these fluids at evaporating and condensing temperatures.) We may further note that the order of the six studied refrigerants will be reversed if we list them according to their theoretical vapor compression cycle COP. Hence, the theoretical COP disadvantage of high-pressure refrigerants can be mitigated through the optimized design of the evaporator and condenser.

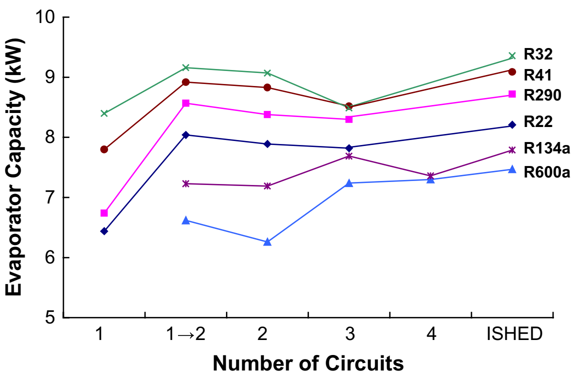

Fig. 6. Evaporator capacities for manually developed and ISHED-optimized circuitry designs (taken from [6]). 1 → 2 denotes a single circuit splitting into two.

5.2. Results for non-uniform inlet air distribution

Cross-flow air-cooled condensers are generally subject to airflow that is non-uniform. For condensers used in split residential air conditioners, the fan is generally located near the top of the assembly with perpendicular orientation with

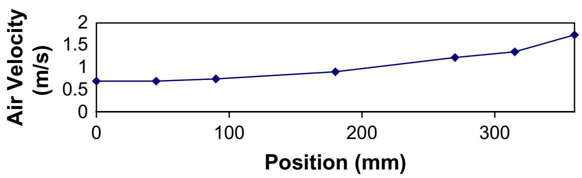

Fig. 7. Non-uniform airflow distribution.

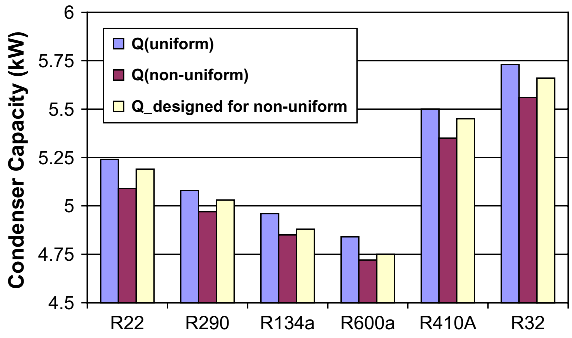

Fig. 8. Recovery of lost condenser capacity from airflow maldistribution with ISHED-optimized circuitries.

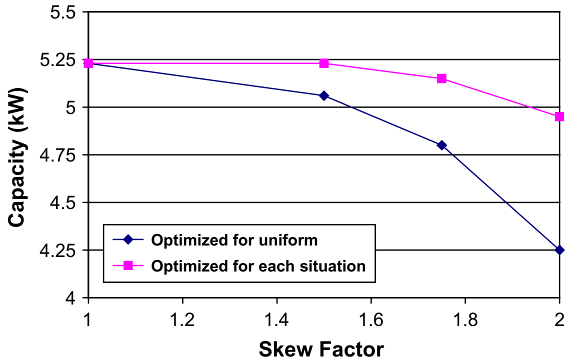

Fig. 9. Condenser capacities of best circuitry for uniform air subject to non-uniform flow compared to optimized for individual airflow profiles.

respect to the coil. This results in greater amount of airflow near the top of the coil. It is therefore interesting to examine ISHED's effectiveness in designing condensers subjected to a non-uniform airflow distribution.

For this task, we took airflow distribution measurements on a typical outdoor condensing unit, and scaled them to the size of the condenser and the volumetric airflow rate of 0.508 $m^3 s^{-1}$ used in this study. Fig. 7 depicts the air velocity profile, with the position measured from the bottom of the condensing unit.

We simulated the performance of each refrigerant in the condenser optimized for uniform airflow using this non-uniform airflow profile. In every case the capacity was less than the capacity with uniform air. We then redesigned each coil with ISHED using this non-uniform air velocity profile as input. The new ISHED designs were able to recover a portion of the lost capacity in every case. Fig. 8 shows the results of these simulations.

As the airflow profile becomes less uniform, optimizing refrigerant circuitry becomes more important. To demonstrate this point, we performed a set of simulations for an R22 condenser with a set of simple linear air velocity profiles. All these air velocity profiles had a total volumetric flow rate of 0.508 $m^3 s^{-1}$ (the same as in the previous simulations), but had a different height-wise velocity gradient. We defined the magnitude of this non-uniformity by the skew factor, S; $S = 1$ for uniform airflow of 1 $m\,s^{-1}$, $S = 2$ for zero flow on one side of the condenser linearly increasing to 2 $m\,s^{-1}$ flow on the opposite side.

Fig. 9 shows the capacities for the different inlet air distributions. The bottom line represents the capacities of the condenser that was optimized for the uniformly distributed air. The upper line represents the capacities of the condenser whose refrigerant circuitry was optimized for each individual air distribution. The figure demonstrates that a large portion of the capacity lost due to airflow non-uniformity can be recovered through optimized circuitry design.

Fig. 10 presents the refrigerant circuitry design generated by ISHED for the extreme case studied, which had zero airflow at the far left side of the coil with the velocity increasing linearly to 2 $m\,s^{-1}$ at the right side. This design has two inlets and one outlet, but the two inlet circuits have different lengths; 12 tubes for one circuit and 8 for the other. Even an experienced engineer would have difficulty assigning

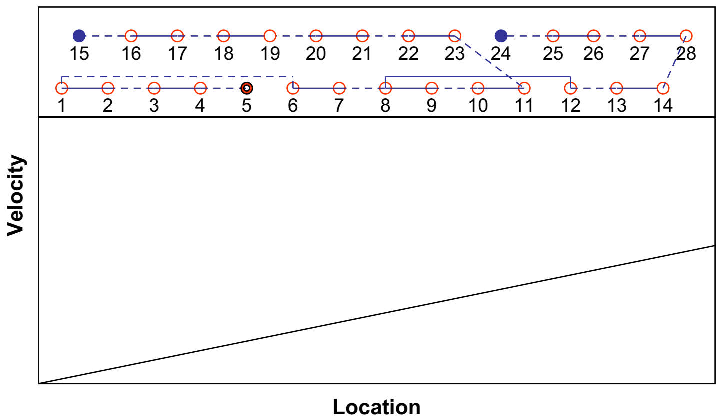

Fig. 10. ISHED-developed circuitry design for linear airflow profile with skew factor $S = 2$.

the best number of tubes per circuit and locating the merging point to maximize the coil capacity for such a non-uniform air velocity profile.

6. Conclusions

We examined the application of ISHED to optimizing refrigerant circuits in finned-tube condensers. For given operating parameters and technical constraints, the ISHED system was able to generate optimized circuitry architectures that were as good as or better than those prepared manually. ISHED was particularly superior in optimizing circuitry architectures for operating cases with non-uniform air velocity profile. Since maximizing capacity is the only objective of ISHED, its designs typically need to be manually modified by a design engineer to accommodate manufacturing constraints. The ISHED optimization system is not constrained by the refrigerant or heat transfer surfaces used other than the limitations imposed by the heat exchanger simulator.

Optimization runs with R600a, R134a, R290, R22, R410A and R32 showed that high-pressure refrigerants benefited from more restrictive circuitry architectures than the low-pressure R600a and R134a. The ratio of condenser capacity for the best performer, R32, and the worst performer, R600a, was 1.18. The superior heat exchanger performance of high-pressure refrigerants renders the opportunity to mitigate their inherent theoretical COP disadvantage in the vapor compression cycle as compared to low-pressure fluids.

References

[1] M. Chwalowski, D.A. Didion, P.A. Domanski, Verification of evaporator computer models and analysis of performance of an evaporator coil, ASHRAE Transactions 95 (1) (1989) (Paper No. CH-89-23-1).
[2] E. Granryd, B. Palm, Optimum number of parallel sections in evaporators, in: Proceedings of the 21st International Congress of Refrigeration, paper ICR0077, Washington, DC, USA, 2003.
[3] S.Y. Liang, T.N. Wong, G.K. Nathan, Numerical and experimental studies of refrigerant circuitry of evaporator coils, International Journal of Refrigeration 24 (8) (2001) 823–833.
[4] V. Casson, A. Cavallini, L. Cecchinato, D. Del Col, L. Doretti, E. Fornasieri, L. Rossetto, C. Zilio, Performance of finned coil condensers optimized for new HFC refrigerants, ASHRAE Transactions 108 (2) (2002) 517–527.
[5] A. Cavallini, D. Del Col, L. Doretti, L. Rossetto, Condensation heat transfer of new refrigerants: advantages of high pressure fluids, in: Proceedings of the Eighth International Refrigeration Conference, Purdue University, West Lafayette, IN, USA, 2000.
[6] P.A. Domanski, D. Yashar, K.A. Kaufman, R.S. Michalski, Optimized design of finned-tube evaporators using learnable evolution methods, International Journal HVAC&R Research 10 (2) (2004) 201–212.
[7] P.A. Domanski, D. Yashar, M. Kim, Performance of a finned-tube evaporator optimized for different refrigerants and its effect on system efficiency, International Journal of Refrigeration 28 (6) (2005) 820–827.
[8] NIST, EVAP–COND – simulation models for finned-tube heat exchangers, National Institute of Standards and Technology, Gaithersburg, MD, USA, 2003. http://www2.bfrl.nist.gov/software/evap-cond/.
[9] P.A. Domanski, W.V. Payne, II, Properties and cycle performance of refrigerant blends operating near and above the refrigerant critical point, Task 2: air conditioner system study, Final report, ARTI-21CR/605-50010-01-Pt. 2, September 2002, 151 pp.
[10] H. Müller-Steinhagen, K. Heck, A simple friction pressure drop correlation for two-phase flow in pipes, Chemical Engineering Process 20 (6) (1986) 297–308.
[11] I.E. Idelchik, Handbook of Hydraulic Resistance, second ed., Hemisphere, New York, NY, USA, 1986.
[12] E.W. Lemmon, M.O. McLinden, M.L. Huber, NIST Reference Fluids Thermo-dynamic and Transport Properties – REFPROP 7.0, Standard Reference Database 23, National Institute of Standards and Technology, Gaithersburg, MD, USA, 2002.
[13] ASHRAE, Designation and Safety Classification of Refrigerants (ANSI/ASHRAE Standard 34-2001), American Society of Heating, Refrigerating, and Air-conditioning Engineers, Atlanta, GA, USA, 2001.
[14] J.M. Calm, G.C. Hourahan, Refrigerant data summary, Engineered Systems 18 (11) (2001) 74–88.
[15] IPCC, Climate change 2001: the scientific basis – contribution of working group I to the IPCC third assessment report, Intergovernmental Panel on Climate Change of the World Meteorological Organization and the United Nations Environment Programme (UNEP), Cambridge University Press, Cambridge, UK, 2001.